Dalton
www.rsc.org/dalton

Thermodynamic and kinetic studies on the Cu^{2+} coordination chemistry of a novel binucleating pyridinophane ligand †

Pilar Díaz,[a] Manuel García Basallote,*[b] M[a] Angeles Máñez,[b] Enrique García-España,*[a] Laura Gil,[a] Julio Latorre,[a] Conxa Soriano,[c] Begoña Verdejo[c] and Santiago V. Luis*[d]

[a] *Departamento de Química Inorgánica, Universidad de Valencia, C/Dr. Moliner 46100, Burjassot (Valencia), Spain. E-mail: enrique.garcia-es@uv.es*

[b] *Departamento de Ciencia de Materiales e Ingeniería Metalúrgica, Facultad de Ciencias, Universidad de Cádiz, Apartado 40, Puerto Real, 11510 Cádiz, Spain*

[c] *Departamento de Química Orgánica, Facultad de Farmacia, Universidad de Valencia, Avda. Vicente Andrés Estellés s/n, 46100, Burjassot (Valencia), Spain*

[d] *Departamento de Química Inorgánica y Orgánica, Universitat Jaume I, 12080, Castellón, Spain*

Received 18th September 2002, Accepted 28th January 2003
First published as an Advance Article on the web 11th February 2003

The synthesis and coordination chemistry of the novel pyridine-functionalized ligand 2,6,9,12,16-pentaaza[17]-(2,6)pyridinophane (**L**[1]) is described. The compound behaves as a hexaprotic base in aqueous solution. NMR studies indicate a protonation pattern in which the sp^2 pyridine nitrogen (N(py)) does not undergo a net protonation although it is involved in formation of hydrogen bonds. **L**[1] forms mono and binuclear hydroxylated complexes. The crystal structure of $[Cu\mathbf{L}^1](ClO_4)_2$ shows a square planar coordination for Cu^{2+} with the pyridine and the three central nitrogens of the chain forming the vertices of the square. The benzylic nitrogens could be occupying the axial positions of a strongly axially asymmetrically elongated octahedron. The kinetic data show that decomposition of the $[Cu(H\mathbf{L}^1)]^{3+}$, $[Cu(\mathbf{L}^1)]^{2+}$ and $[Cu_2(\mathbf{L}^1)(OH)]^{3+}$ complexes takes place in two steps the slower one being ascribed to the dissociation of the Cu–N(py) bond.

Introduction

In recent years we have been involved in the preparation and study of new families of ligands built up by linking together both ends of a polyamine bridge and a variety of aromatic spacers through methylene carbons. The aromatic spacers used were benzene, durene, naphthalene, thiophene, biphenyl or anthracene based moieties (Chart 1).[1–5] One of the most interesting aspects of the coordination chemistry of these compounds is their capability to define coordinatively unsaturated metal sites. The presence of the aromatic spacer precludes the simultaneous coordination of both benzylic nitrogen atoms to the same metal ion leaving vacant positions in the coordination sphere that can be occupied by labile ligands in the reaction medium. Moreover, if the number of nitrogen atoms and the size and flexibility of the polyamine chain are appropriately balanced, formation of binuclear complexes with two coordinatively unsaturated sites can be achieved. This situation is illustrated in the crystal structure of the binuclear complexes of the macrocycles with benzene or naphthalene spacers and the tetramine 1,4,7,10-tetraazadecane (**L**[2] and **L**[3] in Chart 1).[3,4]

The topology and relative rigidity of these ligands leads to the arrangement of the polyamine bridge in two well-separated ethylenediamine subunits each able to coordinate a Cu^{2+} ion. All these metal complexes with open coordination sites, particularly the binuclear ones, are of interest from different points of view including the possibility of catalytically assisting hydrolytic or redox processes.[5]

However, in order to avoid any possible metal dissociation throughout the process, improved complexes displaying higher stabilities are often required. In order to accomplish such requisites, we have constructed the ligand **L**[1] incorporating a pyridine ring linked in positions 2 and 6 through methylene carbon atoms to the pentamine 1,5,8,11,15-pentaazadecane (**L**, 3,2,2,3-pent).[6] The well-known coordinative features of the pyridine nitrogen,[7–16] conjointly with the five amine nitrogens of the bridge and the geometrical features of the ligand could satisfy the expected requirements.

In this first report on the chemistry of this new compound, we describe its synthesis together with a solution study on its ability to form Cu^{2+} complexes. Additionally, we analyze the kinetics of dissociation of the Cu^{2+} complexes, an aspect much

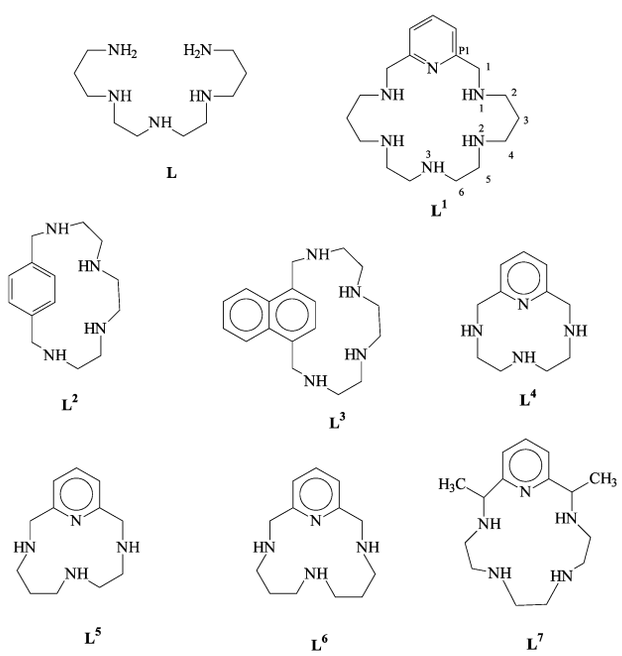

Chart 1

† Electronic supplementary information (ESI) available: Table S1: observed rate constants for the acid-promoted decomposition of Cu^{2+} complexes with ligand **L**. Table S2: observed rate constants for the acid-promoted decomposition of Cu^{2+} complexes with macrocycle **L**[1]. Fig. S1: Variation of some selected ^{13}C chemical shifts as a function of pH. See http://www.rsc.org/suppdata/dt/b2/b209013a/

DOI: 10.1039/b209013a

less covered in the literature, and we compare the data with the relevant results for the open-chain counterpart **L**. We also report on the crystal structure of the complex $[Cu\mathbf{L}^1](ClO_4)_2$.

Experimental

Synthesis

Ligand **L** was prepared as reported in the literature,[6] and was purified by twice crystallizing its hydrobromide salt.

2,6,9,12,16-Pentakis(*p*-tolylsulfonyl)-2,6,9,12,16-pentaaza[17]-2,6-pyridinophane ($\mathbf{L}^1$·5Ts)

A solution of 2,6-bis(bromomethyl)pyridine (3.8 mmol) in 165 mL of CH_2Cl_2–CH_3CN (1 : 1) was added dropwise to a suspension of 1,5,8,11,15-pentakis(*p*-toluensulfonyl)-1,5,8,11,15-pentaazapentadecane (3.8 mmol) and K_2CO_3 (5 g, 37.7 mmol) in 85 mL of CH_3CN. After the addition, the mixture was allowed to reflux for 24 h. Then, the solution was filtered and concentrated. The solid obtained was recrystallized from AcOEt–hexane (1 : 1). Yield: 49%, mp: 210–212 °C. FAB mass spectrum: *m*/*z* 1091 ($[M + H]^+$). ^{1}H NMR ($CDCl_3$), δ 1.69–1.84 (m, J = 7 Hz, 4H), 2.42 (s, 12H), 2.45 (s, 3H), 3.01 (t, J = 8 Hz, 4H), 3.06 (t, J = 8 Hz, 4H), 3.23 (t, J = 8 Hz, 4H), 3.36 (t, J = 8 Hz, 4H), 4.32 (s, 4H), 7.27 (d, J = 8 Hz, 2H), 7.31 (d, J = 8 Hz, 8H), 7.33 (d, J = 8 Hz, 2H), 7.49 (t, J = 8 Hz, 1H), 7.59 (d, J = 8 Hz, 4H), 7.65 (d, J = 8 Hz, 4H), 7.68 (d, J = 8 Hz, 2H). ^{13}C NMR ($CDCl_3$), δ 21.7, 28.8, 48.4, 48.5, 48.7, 49.6, 55.3, 121.5, 127.2, 127.6, 130.0, 130.1, 135.0, 137.8, 143.7, 143.8, 157.2.

2,6,9,12,16-Pentaaza[17]-2,6-pyridinophane hexahydrobromide dihydrate ($\mathbf{L}^1$·6HBr·2H$_2$O)

The tosyl groups of $\mathbf{L}^1$·5Ts (1.8 mmol) were removed by reductive cleavage with a mixture of 195 mL of HBr–AcOH and PhOH (3.5 g, 37.2 mmol) heating at 90 °C for 24 h. Then the solid obtained was filtered off and washed with EtOH–CH_2Cl_2 (1 : 1). The macrocycle was obtained in its hydrobromide form. Yield: 70%. Mp 290–292 °C. Anal. Calc. for $C_{17}H_{32}N_6$·6HBr·2H$_2$O: C, 24.2; H, 5.0; N, 10.0. Found: C, 24.2; H, 5.2; N, 9.8%. ^{1}H NMR (D_2O), δ 2.25 (m, 4H), 3.32 (t, J = 6 Hz, 4H), 3.40 (t, J = 8 Hz, 4H), 3.55 (m, 8H), 4.37 (s, 4H), 7.33 (d, J = 8 Hz, 2H), 7.80 (t, J = 8 Hz, 1H). ^{13}C NMR (D_2O), δ 22.8, 42.2, 42.6, 44.2, 44.9, 51.37, 123.1, 139.4, 150.7.

X-Ray crystallography

Crystals of $[Cu\mathbf{L}^1](ClO_4)_2$ were grown by slow evaporation of a 0.15 mol dm^{-3} $NaClO_4$ aqueous solution containing $Cu(ClO_4)_2$ and $\mathbf{L}^1$·6HBr·2H$_2$O in 1 : 1 molar ratio (0.01 mol dm^{-3} concentrations) and at pH 10. Calc. for $C_{17}H_{31}Cl_2CuN_6O_8$: C, 35.1; H, 5.4; N, 14.4. Found: C, 34.9; H, 5.2; N, 14.6%.

Crystal data and details of the data collection for $[Cu\mathbf{L}^1](ClO_4)_2$ are given in Table 1. Analysis on single crystals of $[Cu\mathbf{L}^1](ClO_4)_2$ was carried out with an Enraf-Nonius CAD-4 single crystal diffractometer. The unit cell dimensions were measured from the angular setting of 25 reflections with θ between 15 and 25°.

The ω–2θ scan technique and a variable scan rate with a maximum scan time of 60 s per reflection were used. The intensity of the primary beam was checked throughout the data collection by monitoring three standard reflections every 3600 s. The final drift corrections factors were in the range 0.98–1.02. Profile analysis was performed on all reflections.[17] A semi-empirical, Ψ-scan based, absorption correction was performed.[18] Lorentz and polarisation corrections were applied and the data were reduced to F_o^2 values. The structure was solved by the Patterson method using the program SHELXS-86 running on an IBM PENTIUM II 300 computer.[19] Isotropic least-squares refinement was performed by means of the program SHELXL-93.[20] Hydrogen atoms were placed in calculated positions. Atomic scattering factors were taken from the International Tables for X-ray Crystallography.[21] The molecular plots were produced by the program ORTEP.[22]

CCDC reference number 194482.

See http://www.rsc.org/suppdata/dt/b2/b209013a/ for crystallographic data in CIF or other electronic format.

Table 1 Crystal data and structure refinement for $[Cu\mathbf{L}^1](ClO_4)_2$

Empirical formula	$C_{17}H_{31}Cl_2CuN_6O_8$
Formula weight	582.93
Temperature/K	293(2)
Wavelength/Å	0.71073
Crystal system	Monoclinic
Space group	$P2_1/n$
a/Å	12.427(5)
b/Å	13.143(5)
c/Å	16.662(5)
β/°	110.000(5)
V/Å^3	2557(2)
Z	4
D_c/g cm^{-3}	1.512
μ/mm^{-1}	0.484
F(000)	1208
Crystal size/mm	0.20 × 0. 15 × 0.10
θ range/°	1–25
Limiting indices	$0 \le h \le 14$ $0 \le k \le 15$ $-19 \le l \le 18$
Reflections collected/unique	4630/4415 [R(int) = 0.1798]
Refinement method	Full-matrix least-squares on F^2
Data/restraints/parameters	4415/0/346
Goodness-of-fit on F^2	0.755
Final R indices [$I > 2\sigma(I)$]	R_1 = 0.0883, wR_2[a] = 0.2259
R indices (all data)	R_1 = 0.1205, wR_2[a] = 0.2715
Largest diff. peak and hole/e Å^{-3}	2.123 and −1.403

[a] $w = 1/[\sigma^2(F_o^2) + (0.2537P)^2 + 12.86P]$ where $P = (\mathrm{Max}(F_o^2) + 2F_c^2)/3$.

Emf measurements

The potentiometric titrations were carried out at 298.1 ± 0.1 K using 0.15 mol dm^{-3} $NaClO_4$ as supporting electrolyte. The experimental procedure (burette, potentiometer, cell, stirrer, microcomputer, *etc.*) has been fully described elsewhere.[23] The acquisition of the emf data was performed with the computer program PASAT.[24] The reference electrode was an Ag/AgCl electrode in saturated KCl solution. The glass electrode was calibrated as an hydrogen-ion concentration probe by titration of previously standardised amounts of HCl with CO_2-free NaOH solutions and determining the equivalent point by the Gran method,[25] which gives the standard potential, $E°'$, and the ionic product of water (pK_w = 13.73(1)).

The computer program HYPERQUAD was used to calculate the protonation and stability constants.[26] The pH range investigated was 2.5–10.5 and the concentration of the Cu^{2+} metal ion and of ligand ranged from 1×10^{-3} to 5×10^{-3} mol dm^{-3} with Cu^{2+} : ligand molar ratios varying from 2 : 1 to 1 : 2. The different titration curves for each system (at least two) were treated either as a single set or as separated curves without significant variations in the values of the stability constants. Finally, the sets of data were merged together and treated simultaneously to give the final stability constants.

NMR measurements

The ^{1}H and ^{13}C NMR spectra were recorded on Varian UNITY 300 and UNITY 400 spectrometers, operating at 299.95 and 399.95 MHz for ^{1}H and at 75.43 and 100.58 MHz for ^{13}C. The spectra were obtained at room temperature in D_2O or $CDCl_3$ solutions. For the ^{13}C NMR spectra dioxane was used as a reference standard (δ = 67.4 ppm) and for the ^{1}H spectra the solvent signal was used. Adjustments to the desired pH were

Table 2 Logarithms of the stepwise protonation constants for ligand $\mathbf{L^1}$ determined in 0.15 mol dm^{-3} $NaClO_4$ at 298.1 K. The protonation constants for **L** (ref. 30) are also included

Reaction[a]	$\mathbf{L^1}$	**L**
$H + L = HL$	9.65(2)[b]	10.55
$H + HL = H_2L$	9.32(1)	9.89
$H + H_2L = H_3L$	7.62(2)	8.69
$H + H_3L = H_4L$	6.62(2)	7.55
$H + H_4L = H_5L$	2.86(3)	3.55
$\log\beta$	36.1	40.2

[a] Charges omitted for clarity. [b] Values in parentheses are standard deviations in the last significant figure.

Table 3 Logarithms of the stepwise stability constants for the formation of Cu^{2+} complexes by receptor $\mathbf{L^1}$ determined in 0.15 mol dm^{-3} $NaClO_4$ at 298.1 K. The stability constants for the system Cu^{2+}–**L** (ref. 30) are also included

Reaction[a]	$\mathbf{L^1}$	**L**
$Cu + L = CuL$	20.44(3)[b]	21.28(2)
$CuL + H = CuHL$	6.96(1)	8.86(1)
$CuHL + H = CuH_2L$	2.75(4)	3.39(2)
$2Cu + L + H_2O = Cu_2L(OH) + H$	20.65(2)	
$2Cu + L + 2H_2O = Cu_2L(OH)_2 + 2H$	10.84(5)	

[a] Charges omitted for clarity. [b] Values in parentheses are standard deviations in the last significant figure.

made using DCl or NaOD solutions. The pH was calculated from the measured pD values using the correlation, pH = pD − 0.4.[27]

Kinetic experiments

The kinetics of decomposition of the mono and binuclear Cu^{2+} complexes with the ligands **L** and $\mathbf{L^1}$ were carried out at 298.1 ± 0.1 K using an Applied Photophysics SX17MV stopped-flow instrument. The solutions used in the kinetic work were prepared by dissolving weighed amounts of the desired ligand and then adding the volume of a stock solution of Cu^{2+} required to achieve the desired Cu : ligand molar ratio. In this way, solutions with 1 : 1 or 2 : 1 ratios (Cu : ligand) were prepared and the pH was then adjusted to values where a single mono- or binuclear species exists. These starting solutions, with a total concentration of the ligand of 1.0×10^{-3} mol dm^{-3}, were mixed in the stopped flow instrument with titrated HNO_3 solutions of different concentrations, the final ionic strength being maintained at 0.10 mol dm^{-3} with KNO_3. All kinetic experiments were carried out under pseudo-first order conditions of acid excess. Preliminary kinetic work using a diode array detector revealed that decomposition of all the complexes studied in this work occurs in one or two separate kinetic steps. In any case, the values derived for the rate constants were independent of the concentration of the starting complex, which shows that the order of reaction with respect to the complex is always one. In cases where decomposition occurs in two steps, preliminary experiments showed that similar values are obtained for the rate constants using either single- or multi-wavelength detection. For this reason, most measurements were carried out at a fixed wavelength of 575 nm (**L** complexes), 590 nm (mononuclear $\mathbf{L^1}$ complexes) or 615 nm (binuclear $\mathbf{L^1}$ complex). All the kinetic traces were well fitted by a single or a double exponential using the standard software of the instrument. The reported values of the rate constants correspond to the mean of six measurements, the standard deviation being always lower than 5%.

Results and discussion

Protonation studies

Table 2 includes the stepwise protonation constants of $\mathbf{L^1}$ conjointly with those previously reported for the open-chain counterpart **L**.[30] The first point that deserves comment is that just five protonation steps can be identified in the pH range of study (2–11).

This most likely implies that there is not a net protonation step involving the pyridine nitrogen atom that suffers a considerable reduction in basicity relative to pyridine itself or analogous compounds of open-chain topology. Similar results have been reported for the related tri- or tetra-aza pyridinophanes $\mathbf{L^4}$–$\mathbf{L^6}$.[8] Apart from this, the stepwise constants follow the trend that should be expected on the basis of minimization of electrostatic repulsion between same sign charges.

$\mathbf{L^1}$ presents two large constants for the first two protonations, two intermediate ones for the third and fourth protonations and one much more reduced value for the last step in which the incoming proton should bind the central nitrogen of the chain surrounded by two protonated sites separated by ethylenic chains.

The results obtained for the open-chain polyamine **L** are parallel, although a greater basicity is observed in all its protonation steps in correspondence with its higher flexibility and ability to separate the positive charges.

^1H and ^{13}C NMR spectra of $\mathbf{L^1}$ at variable pH give also some information about the average protonation scheme of $\mathbf{L^1}$. Particularly, the quaternary carbon atom CP1 in β-position[28,29] relative to nitrogen N1 serves as a probe for identifying the protonation state of this atom (for labelling see Chart 1). The signal of CP1 moves continuously upfield (6.5 ppm) from pH 12 to 5, when the fourth proton binds $\mathbf{L^1}$ (Fig. S1 in the ESI †).

The signal attributed to C1, in α-position with respect to N1, undergoes an analogous although smaller upfield shift (2.3 ppm) in this pH range. These NMR data suggest that two out of the first four protonation steps are affecting the benzylic nitrogen atoms.

Analogously, the large upfield shifts undergone by C5 ($\Delta\delta$ = 4.5 ppm) and downfield shift of the ^1H NMR signal of H6 ($\Delta\delta$ = 0.75 ppm), in β- and α-position relative to N3, respectively, below pH 5 would suggest that the last protonation occurs at the central nitrogen of the chain.

Cu^{2+} complex speciation studies

Table 3 gathers the stability constants, determined by means of pH-metric titration at 298.1 K in 0.15 mol dm^{-3} $NaClO_4$, for the species formed in the system Cu^{2+}–$\mathbf{L^1}$, together with those for the system Cu^{2+}–**L** previously reported.[6,30] $\mathbf{L^1}$ forms mononuclear species $[CuH_j\mathbf{L^1}]^{(2+j)}$ (j = 0–2) as well as the hydroxylated binuclear species $[Cu_2\mathbf{L^1}(OH)]^+$ and $[Cu_2\mathbf{L^1}(OH)_2]^{2+}$.

The nuclearity of the species formed is highly dependent on the molar ratio M : L and while for 1 : 1 ratios only mononuclear species are detected in the whole pH range studied, for 2 : 1 ratios the binuclear hydroxylated ones are the only existing species in solution above pH 6 (Fig. 1).

Although deriving coordination numbers just from free energy terms can be often misleading, a careful consideration of the protonation constants of the complexes as well as comparison with related systems may be useful in some instances. In this sense, as it can be seen in Table 3, the first protonation of the complex $[Cu\mathbf{L^1}]^{2+}$ is characterized by a large constant. This constant compares well with the third protonation step of the free ligand (Table 2), a step in which the reaction displays the same overall charge, and suggests an incomplete participation of the nitrogen donors in the coordination to the metal. This conclusion is in agreement with the crystal structure of the complex that shows two weakly coordinating amino groups (*vide infra*). On the other hand, the stability constant obtained for $[Cu\mathbf{L^1}]^{2+}$ is very close to that of the related complex $[Cu\mathbf{L}]^{2+}$, for which a coordination of four was ascertained by a variety of methods.[6,30] Comparison with the stability data for the Cu^{2+} complexes of 2,6-pyridinophanes containing triamine bridges

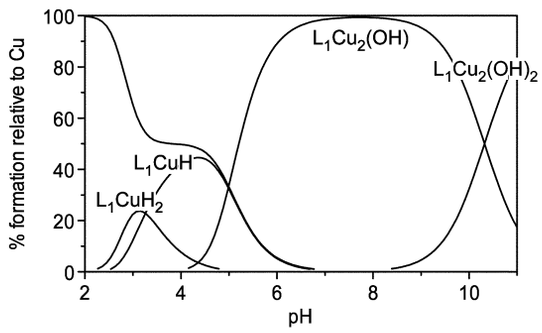

B

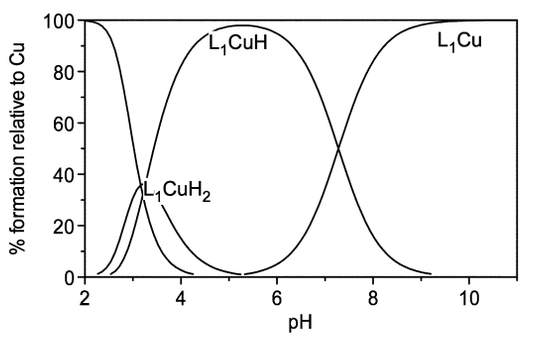

A

Fig. 1 Distribution diagram for the system Cu^{2+}–**L**^{1}: (A) $[Cu^{2+}] = [\mathbf{L}^1] = 10^{-3}$ mol dm^{-3}. (B) $[Cu^{2+}] = 2 \times 10^{-3}$ mol dm^{-3}, $[\mathbf{L}^1] = 10^{-3}$ mol dm^{-3}.

L^4, **L**^{5} and **L**^{6} reveal similar stability although slightly lower than for **L**^{1} ($[Cu\mathbf{L}^4]^{2+}$, $\log K = 20.14$, ($[Cu\mathbf{L}^5]^{2+}$, $\log K = 18.62$, $[Cu\mathbf{L}^6]^{2+}$, $\log K = 19.76$).[9] Therefore, all these data support a likely coordination number of four in this system. However, a larger coordination number (five or six) with a loose participation of the axial ligands could also be invoked to interpret our solution data.

Moreover, the electronic spectrum of $[Cu\mathbf{L}^1]^{2+}$ shows a broad band at *ca.* 590 nm typical of highly distorted octahedral CuN_6 chromophore[31] and strongly suggests that the structure in solution is similar to that in the solid state. The spectrum of $[CuH\mathbf{L}^1]^{3+}$ is very similar to that of $[Cu\mathbf{L}^1]^{2+}$ and suggests a similar geometry. Probably, protonation of one of the loosely bound nitrogens in $[Cu\mathbf{L}^1]^{2+}$ is accompanied by the weak coordination of a water molecule without any important change in the splitting of the d orbitals of the metal ion.

The most appealing aspect of this system is the formation of binuclear hydroxylated complexes. As the ligand donor just has six nitrogen donor atoms one of them being the pyridine sp^2 nitrogen, the ligand by itself cannot saturate the first coordination sphere of the two metal ions that must bind strongly to other ligands such as water molecules. This is revealed by the ready hydrolysis of the bound water molecules that makes $[Cu_2\mathbf{L}^1(OH)]^{3+}$ the prevailing species above pH 5 and $[Cu_2\mathbf{L}^1(OH)_2]^{2+}$ predominant above pH 10.5 (Fig. 1B). The pH values at which hydrolysis occur in the binuclear complexes, suggest a possible coordination of the hydroxo groups as bridging ligands between both metal ions. The electronic spectrum of these species shows a broad band centered at 615 nm, thus showing a significant shift with respect to the mononuclear complexes. Although a definite conclusion about the coordination environment of the metal ions cannot be achieved from the electronic spectrum alone, the red-shift is consistent with a structure similar to the mononuclear species in which some of the nitrogen donors have been replaced by oxygens.[31]

Table 4 Selected bond lengths [Å], angles and torsion angles [°] for $[Cu\mathbf{L}^1](ClO_4)_2$

Cu(1)–N(3)	2.025(7)	Cu(1)–N(4)	2.112(6)
Cu(1)–N(5)	2.041(6)	Cu(1)–N(1)	2.398(6)
Cu(1)–N(2)	2.066(6)	Cu(1)–N(6)	2.549(7)
N(5)–Cu(1)–N(4)	102.6(3)	N(4)–Cu(1)–N(1)	91.7(2)
N(3)–Cu(1)–N(4)	84.1(3)	N(3)–Cu(1)–N(6)	107.4(3)
N(3)–Cu(1)–N(2)	81.2(3)	N(5)–Cu(1)–N(6)	71.8(2)
N(5)–Cu(1)–N(2)	92.0(2)	N(2)–Cu(1)–N(6)	94.1(2)
N(3)–Cu(1)–N(1)	104.3(3)	N(4)–Cu(1)–N(6)	87.0(2)
N(5)–Cu(1)–N(1)	77.2(2)	N(1)–Cu(1)–N(6)	147.8(2)
N(2)–Cu(1)–N(1)	95.2(2)		
C2–N1–C1–C20	90.03	N1–C2–C3–C4	72.72
C1–N1–C2–C3	83.98	C2–C3–C4–N2	80.99
C4–N2–C5–C6	78.91	N2–C5–C6–N3	37.07
C5–N2–C4–C3	169.75	N3–C7–C8–N4	46.67
C7–N3–C6–C5	115.24	N4–C9–C10–C11	81.92
C6–N3–C7–C8	174.86	C9–C10–C11–N6	71.89
C8–N4–C9–C10	65.90	N6–C12–C24–N5	28.56
C9–N4–C8–C7	116.52	N6–C12–C24–C23	151.17
C11–N6–C12–C24	81.88	N1–C1–C20–N5	37.64
C12–N6–C11–C10	156.95	N1–C1–C20–C21	143.41

Crystal structure of $[CuL^1](ClO_4)_2$

The crystal structure consists of $[Cu\mathbf{L}^1]^{2+}$ cations and perchlorate counter-anions. The Cu^{2+} presents a highly distorted octahedral geometry. The equatorial plane is defined by the sp^2 pyridine nitrogen and the three central nitrogens of the polyamine chain.

The bond distances in the equatorial plane are quite uniform ranging from 2.020(7) to 2.112(7) Å (Table 4). The Cu^{2+} ion is close to the mean plane defined by the equatorial nitrogens with a largest deviation of only 0.047(1) Å. The angles of the coordination sites are also in accord with this arrangement (Table 4). Additionally, two benzylic nitrogens occupy the axial positions of the very strongly distorted octahedron (Fig. 2, Table 4). The axial distances are Cu–N1 2.398(6) Å and Cu–N(6) 2.549(7) Å. The structure can be interpreted taking into account the participation of the pyridine nitrogen in the coordination sphere and the steric difficulties resulting from both benzyl nitrogens coordinating to the metal ion. The more flexible central part of the molecule can rearrange itself in order to provide the remaining three nitrogens needed to fulfill a square planar coordination around the copper ion. These central nitrogen atoms, particularly the one in the middle (see acid–base section), are

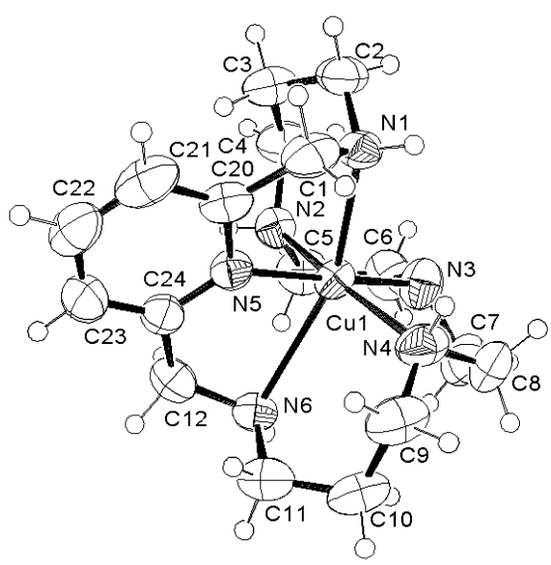

Fig. 2 ORTEP drawing of the cation $[Cu\mathbf{L}^1]^{2+}$. Thermal ellipsoids are drawn at the 30% probability level.

less basic in aqueous solution. This arrangement leads to a difference relative to the crystal structure of the complex $[CuL^7](PF_6)_2$ of the related tetraminic ligand L^7 in which the metal, the pyridine and the two adjacent nitrogens are approximately coplanar and the other two nitrogens are coordinated above and below the plane to give a trigonal-bipyramidal arrangement.[32]

The wrapping of L^1 around the metal ion is manifested in the torsion angles along the polyamine bridge (Table 4). It is interesting to note that the metal ion is almost completely included within the cavity defined by the chain (see the figure in the graphical abstract).

Kinetic measurements

In order to obtain more information about the chemical properties of the Cu^{2+} complexes of L^1, the kinetics of decomposition of these complexes in acidic solution was also studied. The species distribution curves in Fig. 1 show that no Cu^{2+}–L^1 complex exists at pH values lower than *ca.* 2. So, addition of an excess of acid to solutions of the metal complexes will result in complete decomposition with release of Cu^{2+} and protonated ligand. The possible effects caused by both the macrocyclic structure and the presence of coordinated pyridine on the kinetics of decomposition were addressed by comparing the results with those corresponding to the analogous complexes of the open-chain ligand **L**.

According to equilibrium data, the open-chain ligand **L** forms three mononuclear complexes ($[H_2CuL]^{4+}$, $[HCuL]^{3+}$ and $[CuL]^{2+}$) but the concentration of $[H_2CuL]^{4+}$ never represents more than *ca.* 30% of the total amount of ligand. In contrast, the species distribution curves indicate that conditions can be selected in which the $[HCuL]^{3+}$ or $[CuL]^{2+}$ complexes are the only species in solution and so, the kinetics of decomposition of these compounds can be easily studied. Kinetic experiments showed that decomposition of both Cu–**L** complexes occurs in a single kinetic step, and the values derived for the observed rate constant k_{obs} are included in the ESI.† The dependence of k_{obs} with the concentration of acid is linear (Fig. 3) and can be represented by eqn. (1), the value of b being 216(3) mol^{-1} dm^3 s^{-1} for $[HCuL]^{3+}$ and 219(3) mol^{-1} dm^3 s^{-1} for $[CuL]^{2+}$. Thus, the kinetic results for both complexes are quite similar and can be considered to be equivalent within experimental error.

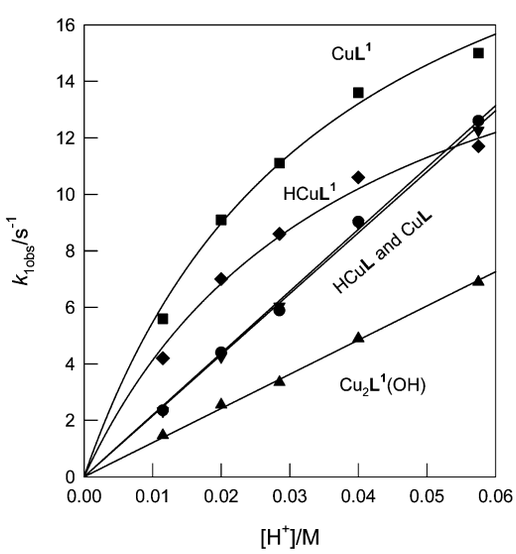

Fig. 3 Plot of the observed rate constant *vs.* the concentration of added acid for the decomposition of Cu^{2+} complexes with ligands **L** and L^1. For the case of the **L** complexes, decomposition occurs in a single step and the plotted values correspond to k_{obs}. For the complexes of L^1 there are two separate kinetic steps and the plotted values correspond to the first step (k_{1obs}).

$$k_{obs} = b[H^+] \quad (1)$$

The species distribution curves for the Cu^{2+} complexes of the macrocyclic L^1 ligand indicate that conditions can be also selected at which a single species ($[HCuL^1]^{3+}$, $[CuL^1]^{2+}$ or $[Cu_2L^1(OH)]^{3+}$) predominate in solution. The decomposition of these complexes upon addition of an excess of acid occurs in two separate kinetic steps and the corresponding values of the observed rate constants k_{1obs} and k_{2obs} are included in the ESI.† The changes in the spectrum with time were also used to calculate the spectrum of the reaction intermediate formed in the first step and Fig. 4 includes the results obtained for the case of $[HCuL^1]^{3+}$. The results for the other complexes were similar; the intermediate showing in all cases a weak band centered at *ca.* 610 nm. The values of k_{1obs} for $[CuL^1]^{2+}$ and $[HCuL^1]^{3+}$ are close to k_{obs} for the related non-macrocyclic complexes, although there is a significant curvature in the plot of the k_{1obs} *vs.* $[H^+]$ data (Fig. 3) that indicates that they must be fitted by eqn. (2). The values so derived for b and c are given in Table 5.

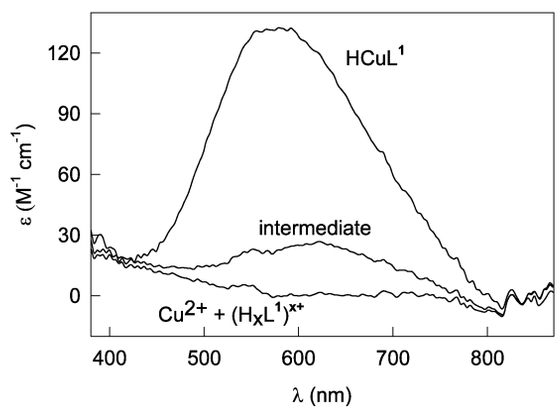

Fig. 4 Calculated spectra for the starting complex ($[HCuL^1]^{3+}$, the reaction intermediate and the final product (Cu^{2+} and protonated L^1) in the decomposition of the $[HCuL^1]^{3+}$ species. These spectra were calculated from the time dependence of the absorption spectra during decomposition.

$$k_{1obs} = \frac{b[H^+]}{1 + c[H^+]} \quad (2)$$

The second kinetic step in the decomposition of the Cu–L^1 complexes is much slower than the first one and the dependence with the concentration of acid is more complex (eqn. (3)) because of the existence of a non-zero intercept (Fig. 5).

$$k_{2obs} = \frac{a + b[H^+]}{1 + c[H^+]} \quad (3)$$

The values of a, b and c obtained for the three complexes are also given in Table 5.

Despite the apparently different rate laws observed for the decomposition of the Cu^{2+} complexes with **L** and L^1, the dependence of the observed rate constants with $[H^+]$ can be represented in all cases by eqn. (3), which has been previously found for the decomposition of complexes with related ligands.[33–41]

This rate law can be interpreted[41–43] in terms of the mechanism depicted in eqns. (4)–(6) that considers the initial formation under steady-state conditions of an activated species (ML)* in which there is a weakening of the Cu–N bond without its replacement by any other ligand. This step is followed by parallel attacks by H^+ and/or the solvent that lead to complex decomposition. From the values of a, b and c, the mechanistically relevant kinetic parameters k_1, k_H/k_{H_2O} and k_{-1}/k_{H_2O} can be calculated[41] and they are also included in Table 5. The

Table 5 Kinetic parameters for the decomposition of the Cu–**L**[1] complexes at 298.1 K and 0.10 mol dm^{-3} KNO_3. The values of *a*, *b* and *c* were obtained by fitting the primary kinetic data to eqns. (1), (2) and (3) in the text. The values of k_1, k_H/k_{H_2O} and k_{-1}/k_{H_2O} were obtained from *a*, *b* and *c* using the equations given in ref. 39 (see footnotes c, e and f)[a]

		$[HCuL^1]^{3+}$	$[CuL^1]^{2+}$	$[Cu_2L^1(OH)]^{3+}$
First kinetic step[b]	$10^{-2}b/M^{-1}\ s^{-1}$	5.2(5)	7.0(6)	1.21(1)
	c/M^{-1}	26(5)	28(4)	
	k_1[c]$/s^{-1}$	20(2)	25(2)	
Second kinetic step	a/s^{-1}	0.04(1)	0.12(5)	0.09(1)
	$10^{-2}\ b/M^{-1}\ s^{-1}$	0.18(2)	0.23(9)	0.06(1)
	c/M^{-1}	44(5)	48(24)	9(2)
	k_1[d]$/s^{-1}$	0.40(1)	0.48(4)	0.76(8)
	$10^{-2}k_H/k_{H_2O}$[e]$/s^{-1}$	5(2)	2(1)	0.7(1)
	k_{-1}/k_{H_2O}[f]	10(3)	3(1)	7.2(5)

[a] The numbers in parentheses represent the standard deviation in the last significant digit. [b] These values are derived from the dependence with $[H^+]$ of k_{1obs}. [c] Calculated as $k_1 = b/c$. [d] These values are derived from the dependence with $[H^+]$ of k_{2obs}. [e] Calculated as $k_H/k_{H_2O} = b/a$. [f] Calculated as $k_{-1}/k_{H_2O} = [b/(a \times c)] - 1$.

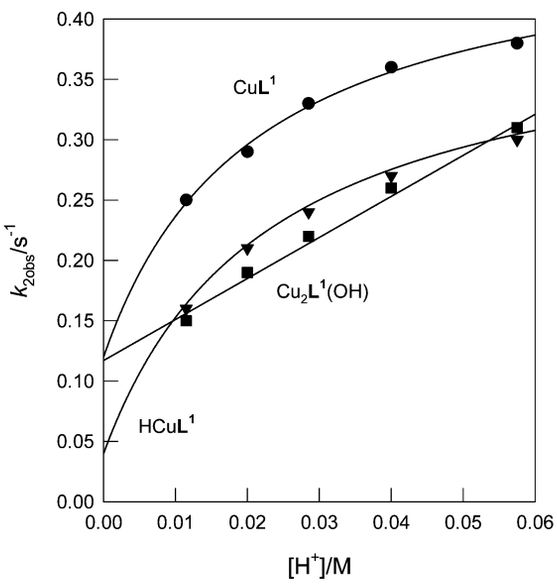

Fig. 5 Plot of k_{2obs} *vs.* the concentration of added acid for the second step in the decomposition of Cu^{2+} complexes with ligand **L**[1].

absence of some terms in the experimental rate laws simply indicates negligible contributions from some of the parallel pathways.

$$ML \rightleftarrows (ML)^* \qquad k_1, k_{-1} \qquad (4)$$

$$(ML)^* + H^+ \longrightarrow M + HL^+ \qquad k_H \qquad (5)$$

$$(ML)^* + H_2O \longrightarrow M + HL^+ \qquad k_{H_2O} \qquad (6)$$

Although the kinetics of decomposition is controlled by the lability of the Cu–N bonds and the rates of attack by H^+ and H_2O, the kinetics of decomposition of Cu^{2+}–polyamine complexes may also show significant changes with the nature of the species.[37,38] However, the similarity of kinetic data for the decomposition of the $[HCuL]^{3+}$ and $[CuL]^{2+}$ complexes of the linear ligand **L** indicates a common rate-determining step in the decomposition of both species. Taking into account all the previous studies on this system,[6,30] a plausible explanation would be to consider that $[CuL]^{2+}$ contains an uncoordinated amine group that would be rapidly protonated to $[HCuL]^{3+}$, thus leading to similar kinetics of decomposition for both complexes.

The values of the mechanistically relevant rate constants in eqns. (4)–(6) have been shown to be strongly dependent on the nature of the metal complexes, especially on the linear-macrocyclic character of the ligand and the number and size of chelate rings affected by nitrogen dissociation.[34,41] For the case of the complexes with the open-chain amine **L**, only the value of *b* is determined, which precludes the determination of k_1 and indicates that attack by H^+ is faster than attack by the solvent ($k_H[H^+] \gg k_{H_2O}$). The numerical value of *b* (2.19×10^2 mol^{-1} dm^3 s^{-1}) is an order of magnitude smaller than the values found for simpler Cu^{2+}–polyamine complexes such as $[Cu(en)]^{2+}$ and $[Cu(dien)]^{2+}$,[35] although it is larger than those corresponding to decomposition of the closely related tetramine complexes $[Cu(3,3,3\text{-tet})]^{2+}$, $[Cu(2,3,2\text{-tet})]^{2+}$ and $[Cu(3,2,3\text{-tet})]^{2+}$.[34]

Moreover, although the values of *b* for $[CuL]^{2+}$ and $[HCuL]^{3+}$ are close to that of $[Cu(2,2,2\text{-tet})]^{2+}$ (1.24×10^2 mol^{-1} dm^3 s^{-1}),[34] in the latter case there is also a significant *a* term (160.3 s^{-1}). Thus, although the kinetics of decomposition of the **L** complexes can be considered intermediate between those of complexes containing only ethylenediamine chelate rings and those containing also propylenediamine rings, an unequivocal correlation between the kinetics of decomposition and the number and type of chelate ring formed can not be established.

As shown in Fig. 3, the values of the rate constant for the first step in the decomposition of the mononuclear macrocyclic complexes $[CuL^1]^{2+}$ and $[HCuL^1]^{3+}$ are close to those of k_{obs} for the non-macrocyclic complexes of **L**, although there is now an additional second step slower than the first one. As the major difference between both ligands is the existence of a coordinated pyridine group in the complexes of **L**[1], it appears reasonable to attribute the slower step to dissociation of the Cu–N(py) bond.

The lower basicity of the aromatic group makes reasonable a slower protonation and, although there are few kinetic data for the decomposition of Cu^{2+} complexes containing both aliphatic and aromatic amine groups, there is literature evidence showing that the dissociation of the aromatic nitrogens is slower.[36,37]

An important difference between the k_{1obs} data for the **L**[1] complexes and k_{obs} for the **L** complexes is the curvature in the plot of the k_{1obs} values *vs.* $[H^+]$. The limiting value of k_{1obs}, which measures the intrinsic lability of the Cu–N bond (k_1), is only 20–25 s^{-1} and extrapolation of the data for the **L** complexes leads to a higher value, which indicates that the Cu–N bonds are less labile in the macrocyclic complexes. This is probably a consequence of the restricted ability of the coordinated amine groups to separate from the metal ion in the macrocyclic complexes and, actually, it has been pointed out that macrocyclic complexes tend to decompose at a slower rate than their open-chain analogues.[38] As a consequence of the curvature in the plots of k_{1obs} *vs.* $[H^+]$, another difference between the Cu^{2+} complexes of **L** and **L**[1] is the appearance of a detectable *c* term in the $[CuL^1]^{2+}$ and $[HCuL^1]^{3+}$ complexes. Although this can be interpreted in terms of a more important contribution of the k_H

pathway in the complexes of $\mathbf{L^1}$, this conclusion is only tentative because the parameter c includes contributions from k_{-1}, $k_{\mathbf{H}}$ and $k_{\mathbf{H_2O}}$.

The comparison of kinetic data for the decomposition of $[Cu\mathbf{L^1}]^{2+}$ and $[HCu\mathbf{L^1}]^{3+}$ reveals small but significant differences (see Fig. 3). These differences clearly indicate that the decomposition of $[Cu\mathbf{L^1}]^{2+}$ does not occur through rapid protonation to give $[HCu\mathbf{L^1}]^{3+}$ followed by rate-determining dissociation of the second Cu–N bond; in contrast, they strongly suggest that the rate of decomposition is controlled in both complexes by dissociation of the first Cu–N bond. According to the crystal structure of $[Cu\mathbf{L^1}](ClO_4)_2$, the ion $[Cu\mathbf{L^1}]^{2+}$ contains two very loosely coordinated amino group and one of them must be protonated in the $[HCu\mathbf{L^1}]^{3+}$ species. The different kinetic results for both complexes indicate that protonation of this group is enough to cause a change in the kinetic properties of the amino groups that remain coordinated. A similar conclusion has been previously reached for ancillary ligands, which play a significant role in the kinetics of decomposition of Cu^{2+} complexes with related macrocyclic polyamine and cryptands.[38,39]

The decomposition of the binuclear $[Cu_2\mathbf{L^1}(OH)]^{3+}$ complex occurs with kinetics very similar to that of the mononuclear $[Cu\mathbf{L^1}]^{2+}$ and $[HCu\mathbf{L^1}]^{3+}$ complexes, although the observed rate constants for both steps are smaller, especially in the case of k_{1obs}. The similarity in the kinetics of decomposition of $[Cu_2\mathbf{L^1}(OH)]^{3+}$ and the related mononuclear complexes could be interpreted in terms of rapid release of the first metal ion followed by rate-determining dissociation of the second Cu^{2+} ion. Nevertheless, this interpretation appears unreasonable in the context of previous kinetic studies of binuclear complexes that showed kinetics of decomposition similar to that of the related mononuclear complexes.[33,38,39] Indeed, the rapid release of the first metal ion should cause an absorbance change within the mixing time of the stopped-flow instrument that has not been observed experimentally. An alternative interpretation would be to consider that the dissociation of the first Cu^{2+} is rate determining and that the second ion is rapidly released. In that case, only the release of the first ion would be monitored and it would occur with a kinetics close to that of $[HCu\mathbf{L^1}]^{3+}$ and $[Cu\mathbf{L^1}]^{2+}$. Although there is no experimental evidence to rule out this possibility, it also appears unlikely because dissociation of the first ion would lead to a mononuclear species that should decompose with a kinetics also similar to that of $[HCu\mathbf{L^1}]^{3+}$ and $[Cu\mathbf{L^1}]^{2+}$.

The most reasonable interpretation to these facts is to consider that decomposition of the binuclear $[Cu_2\mathbf{L^1}(OH)]^{3+}$ complex occurs with statistically controlled kinetics, a possibility that has been previously demonstrated for related binuclear Cu^{2+} complexes.[33,38,39] In that case, the rate of release of the first ion would double the rate of dissociation of the second one and simplification of the kinetic equations lead to the experimental observation only of the dissociation of the second ion.[33] If statistical kinetics is assumed, the values of k_{1obs} for dissociation of the first metal ion in $[Cu_2\mathbf{L^1}(OH)]^{3+}$ would be twice the values in Table S1 (ESI †, which leads to values comparable to those found for $[HCu\mathbf{L^1}]^{3+}$ and $[Cu\mathbf{L^1}]^{2+}$.

The equilibrium measurements indicate that all the six nitrogen donors of $\mathbf{L^1}$ are involved in metal coordination in the binuclear $[Cu_2\mathbf{L^1}(OH)]^{3+}$ complex. Although the structure of this binuclear complex is unknown, the nature of $\mathbf{L^1}$ makes a symmetrical structure with two equivalent Cu^{2+} ions untenable. Because none of the six nitrogen atoms in $\mathbf{L^1}$ is able to form a bridge between the Cu^{2+} centers, each must be then coordinated to one of the metal ions in a dimeric structure bridged by an OH^- group. The observation of statistical kinetics would thus indicate that the rates of attack to the first Cu–NH bond at both metal centers are in the statistical 2 : 1 ratio, thus leading to k_{1obs} values close to those found for the mononuclear complexes. Once dissociated from NH groups, one of the Cu^{2+} ions would be completely released but the second one must contain a Cu–N(py) bond that is attacked at a slower rate, which leads to the observation of a second kinetic step with k_{2obs} values close again to those found for $[HCu\mathbf{L^1}]^{3+}$ and $[Cu\mathbf{L^1}]^{2+}$.

Conclusions

The synthesis of a pyridinophane receptor $\mathbf{L^1}$ able to incorporate two metal ions is presented. NMR studies reveal a protonation scheme in which the nitrogens lining the propylenic chains are involved in the first protonation steps. The crystal structure of $[Cu\mathbf{L^1}](ClO_4)_2$ shows an interesting arrangement of the macrocycle regulated by the flexibility of the chain that allows the pyridine nitrogen and the three central nitrogens of the bridge to be disposed at the corners of a square, with the remaining nitrogens occupying positions leading to a strongly distorted octahedron. The Cu^{2+} speciation studies show the ready formation of binuclear hydroxylated species at relatively low pH values. This characteristic, together with the non-saturated coordination sphere around the metal ions in the binuclear complexes, makes this system suitable for the incorporation of additional guests and for possible use as a catalytic centre. Currently we are exploring these points. Kinetic studies evidence also the different types of nitrogen donors involved in the coordination of Cu^{2+}.

Acknowledgements

We would like to acknowledge Ministerio de Ciencia y Tecnología BQU2000-1424 and BQU2000-0232 for financial support.

References

1 A. Bencini, M. I. Burguete, E. García-España, S. V. Luis, J. F. Miravet and C. Soriano, *J. Org. Chem.*, 1993, **58**, 4749; M. I. Burguete, B. Escuder, E. García-España, S. V. Luis and J. F. Miravet, *J. Org. Chem.*, 1994, **59**, 1067–1071; B. Altava, M. I. Burguete, B. Escuder, S. V. Luis, E. García-España and M. C. Muñoz, *Tetrahedron*, 1997, **53**, 2629.

2 A. Andrés, M. I. Burguete, E. García-España, S. V. Luis, J. F. Miravet and C. Soriano, *J. Chem. Soc., Perkin Trans. 2*, 1993, 749; E. García-España, J. Latorre, S. V. Luis, J. F. Miravet, P. Pozuelo, J. A. Ramírez and C. Soriano, *Inorg. Chem.*, 1996, **35**, 4591; B. Altava, A. Bianchi, C. Bazzicalupi, M. I. Burguete, E. García-España, S. V. Luis and J. F. Miravet, *Supramol. Chem.*, 1997, **8**, 287; J. A. Aguilar, P. Díaz, A. Doménech, E. García-España, J.-M. Llinares, S. V. Luis, J. A. Ramírez and C. Soriano, *J. Chem. Soc., Perkin Trans. 2*, 1999, 1159; M. I. Burguete, P. Díaz, E. García-España, S. V. Luis, J. F. Miravet, M. Querol and J. A. Ramírez, *Chem. Commun.*, 1999, 649.

3 A. Andrés, C. Bazzicalupi, A. Bianchi, E. García-España, S. V. Luis, J. F. Miravet and J. A. Ramírez, *J. Chem. Soc., Dalton Trans.*, 1994, 1995.

4 M. I. Burguete, B. Escuder, E. García-España, J. Latorre, S. V. Luis and J. A. Ramírez, *Inorg. Chim. Acta*, 2000, **300–302**, 970.

5 B. Altava, M. I. Burguete, S. V. Luis, J. F. Miravet, E. García-España, V. Marcelino and C. Soriano, *Tetrahedron*, 1997, **53**, 4751; D. K. Chand, H.-J. Schneider, J. A. Aguilar, F. Escartí, E. García-España and S. V. Luis, *Inorg. Chim. Acta*, 2000, **316**, 71.

6 H. Gamp, D. Haspra, M. Maeder and M. Zuberbuehler, *Inorg. Chem.*, 1984, **23**, 3724.

7 M. G. B. Drew, A. H. Bin Otham, P. D. A. Mcllroy and S. M. Nelson, *J. Chem. Soc., Dalton Trans.*, 1975, 2507; M. G. B. Drew, A. H. Bin Otham, S. G. McFall, P. D. A. Mcllroy and S. M. Nelson, *J. Chem. Soc., Dalton Trans.*, 1977, 1173; M. G. B. Drew, B. P. Murphy, J. Nelson and S. M. Nelson, *J. Chem. Soc., Dalton Trans.*, 1987, 873.

8 H. Adams, N. A. Bailey, D. E. Fenton, W. D. Carlisle and G. Rossi, *J. Chem. Soc., Dalton Trans.*, 1990, 1271.

9 J. Costa and R. Delgado, *Inorg. Chem.*, 1993, **32**, 5257; J. Costa, R. Delgado, M. G. B. Drew, V. Félix, R. T. Henriques and J. C. Waerenborgh, *J. Chem. Soc., Dalton Trans.*, 1999, 3253.

10 G. L. Rothermel Jr., L. Miao, A. L. Hill and S. C. Jackels, *Inorg. Chem.*, 1992, **31**, 4854; L. H. LanBryant Jr., A. Lachgar, K. S. Coates and S. C. Jackels, *Inorg. Chem.*, 1994, **33**, 2219.

11 F. Arnaud-Neu, M. Sanchez and M.-J. Schwing-Weill, *Helv. Chim. Acta*, 1985, **68**, 840.
12 B. Alpha, E. Anklam, R. Deschenaux, J.-M. Lehn and M. Pietraskiewicz, *Helv. Chim. Acta*, 1988, **71**, 1042.
13 J. Casabó, L. Escriche, S. Alegret, C. Jaime, C. Pérez-Jiménez, L. Mestres, J. Rius, E. Molins, C. Miratvilles and F. Teixidor, *Inorg. Chem.*, 1991, **30**, 1893.
14 R. Menif, A. E. Martell, P. J. Squattrito and A. Clearfield, *Inorg. Chem.*, 1990, **29**, 4723.
15 K. E. Krakoviak, J. S. Bradshaw, W. Jiang, N. K. Dalley, G. Wu and R. M. Izatt, *J. Org. Chem.*, 1991, **56**, 2675.
16 K. I. Dhont, G. G. Kerman, A. C. Fabretti, W. Lippens and A. M. Goeminne, *J. Chem. Soc., Dalton Trans.*, 1996, 1753.
17 (*a*) M. S. Lehman and F. K. Larsen, *Acta Crystallogr., Sect. A*, 1974, **30**, 580; (*b*) D. F. Grant and E. J. Gabe, *J. Appl. Crystallogr.*, 1978, **11**, 114.
18 A. C. T. Nort, D. C. Philips and F. S. Mathews, *Acta Crystallogr., Sect. A*, 1968, **24**, 351.
19 G. M. Sheldrick, C. Kruger and R. Goddard (Editors), *Crystallographic Computing*, Clarendon Press, Oxford, England, 1985, p. 175.
20 G. M. Sheldrick, SHELXL-93: Program for Crystal Structure Refinement, Institute fhr Anorgannishe Chemie der Univeritat Göttingen, Germany, 1993.
21 *International Tables for X-ray Crystallography*, The Kynoch Press, Birmingham, England, 1974, vol. IV.
22 C. K. Johnson, ORTEP, Report ORNL-3794, Oak Ridge National Laboratory, Oak Ridge, TN, 1971.
23 E .García-España, M.-J. Ballester, F. Lloret, J.-M. Moratal, J. Faus and A. Bianchi, *J. Chem. Soc., Dalton Trans.*, 1988, 101.
24 M. Fontanelli and M. Micheloni, *Proceedings of the I Spanish–Italian Congress on Thermodynamics of Metal Complexes*, Diputación de Castellón, Castellón, Spain, 1990. Program for the automatic control of the microburette and the acquisition of the electromotive force readings.
25 G. Gran, *Analyst (London)*, 1952, **77**, 881; F. J. Rossotti and H. Rossotti, *J. Chem. Educ.*, 1965, **42**, 375.
26 P. Gans, A. Sabatini and A. Vacca, *Talanta*, 1996, **43**, 1739.
27 A. K. Convington, M. Paabo, R. A. Robinson and R. G. Bates, *Anal. Chem.*, 1968, **40**, 700.
28 J. E. Sarnesky, H. L. Surprenant, F. K. Molen and C. N. Reiley, *Anal. Chem.*, 1975, **47**, 2116.
29 A. Bencini, A. Bianchi, E. García-España, M. Micheloni and J. A. Ramírez, *Coord. Chem. Rev.*, 1999, **88**, 97.
30 J. A. Aguilar, P. Díaz, F. Escartí, E. García-España, L. Gil, C. Soriano and B. Verdejo, *Inorg. Chim. Acta*, 2002, **39**, 307.
31 A. B. P. Lever, *Inorganic Electronic Spectroscopy (Second Edition*), Elsevier: New York 1984, pp. 554.
32 M. G. B. Drew and S. Hollis, *Inorg. Chim. Acta*, 1978, **29**, L231.
33 M. G. Basallote, J. Durán, M. J. Fernández-Trujillo and M. A. Máñez, *J. Chem. Soc., Dalton Trans.*, 1999, 3817.
34 L. H. Chen and C. S. Chung, *Inorg. Chem.*, 1989, **28**, 1402.
35 S. Siddiqui and R. E. Shepherd, *Inorg. Chem.*, 1983, **22**, 3726.
36 R. W. Hay, M. M. Hassan, D. E. Fenton and B. P. Murphy, *Transition Met. Chem.*, 1994, **19**, 559.
37 H. Sun, H. Lin, S. Zhu, G. Zhao, X. Su and Y. Chen, *Polyhedron*, 1999, **18**, 1045.
38 M. G. Basallote, J. Durán, M. J. Fernández-Trujillo and M. A. Máñez, *Polyhedron*, 2001, **20**, 75.
39 M. G. Basallote, J. Durán, M. J. Fernández-Trujillo and M. A. Mañez, *J. Chem. Soc., Dalton Trans.*, 2002, 2074.
40 M. G. Basallote, J. Durán, M. J. Fernández-Trujillo, M. A. Máñez, M. Quirós and J. M. Salas, *Polyhedron*, 2001, **20**, 297.
41 M. J. Fernández-Trujillo, B. Szpoganicz, M. A. Máñez, L. T. Kist and M. G. Basallote, *Polyhedron*, 1996, **15**, 3511.
42 (*a*) R. W. Hay, M. P. Pujari and R. Bembi, *Transition Met. Chem.*, 1986, **11**, 261; (*b*) D. W. Margerum, G. R. Cayley, D. C. Weatherburn and G. Pagenkopt, in *Coordination Chemistry*, vol. 2, p. 1 (edited by A. E. Martell), ACS Monograph 174, American Chemical Society, Washington, DC 1978.
43 R. A. Read and D. W. Margerum, *Inorg. Chem.*, 1981, **20**, 3143.